Microsystem Technologies
https://doi.org/10.1007/s00542-018-4200-z

TECHNICAL PAPER

Ion sensitive field effect transistor based on graphene and ionophore hybrid membrane for phosphate detection

Jungyoon Kim[1] · Li Wang[2] · Tarik Bourouina[3] · Tianhong Cui[1]

Received: 1 October 2018 / Accepted: 13 October 2018

Abstract
This paper reports ion sensitive field effect transistor (IS-FET) with graphene/ionophore hybrid membrane for phosphate detection. CVD graphene is used as a sensing material because the electrical property of graphene can be easily changed by a surrounding condition. In the experiment, a shift of Dirac point is measured to check the concentration of the ions in the water. Since graphene does not have selectivity for the specific ions, phosphate selective membrane is used for the selectivity. The membrane is synthesized by molecular imprinted polymer. To check the selectivity of the graphene sensor coated with the selective membrane, the IS-FET is characterized with several solutions, which have different ions and concentrations. The sensor response is measured by a semiconductor analyzer. Four different ion solutions are used for the measurement (phosphate, sulfate, chloride, and nitrate). Each solution has four different concentrations (0, 0.1, 1 and 10 mg/L). The Dirac point shift from − 0.4 to − 0.2 V as increasing the concentration. The detection limit and response time are 0.1 mg/L and 10 s, respectively.

1 Introduction

Phosphorus is one of the essential elements for growth of plants. However, excessive quantity of phosphorus in water can make eutrophication and decrease water quality. Phosphorus is very toxic and can be accumulated in a living organism. Since phosphate (PO_4^{3-}) is the derivative of phosphorus, detection of phosphate is necessary for quality of water. The allowable maximum concentration of phosphate to avoid accelerated eutrophication is about 0.1 mg/L (Cheng et al. 2010). Many researchers have studied the fabrication of the phosphate ion sensitive sensor to detect the phosphate ion in the water. The commercialized current phosphate detection method is colorimetric standard method, however this method still has some disadvantages (Dickman and Bray 1940). It needs complicate processes such as filtration, calibration and several chemical reaction steps with many reagents before the measurement. Although the current standard methods have a detection limit below the level of the regulation limit, it still needs to be further developed to avoid the time consuming process. Therefore, the investigation of new devices is highly desirable to simplify the measurement.

After the discovery of graphene, various techniques related to graphene family such as graphene oxide and reduced graphene were also studied by many research groups because of the low price (Geim and Novoselov 2007; Kim et al. 2014; Tkachev et al. 2012). However, further technical investigation and applications of graphene have been intensively studied and enhanced with different growth methods, transfer and cleaning process (Zheng et al. 2009; Her et al. 2013; Ahn et al. 2016). The advancement in graphene technology makes it possible to practically applicable in the sophisticated devices including solar cells, organic lighting emitting diode and sensors (Miao et al. 2012; Shin et al. 2013; Kim et al. 2015; Liu et al. 2012). Especially, many researchers who study sensors have focused on graphene due to the superior electrical or mechanical properties of graphene (Du et al. 2011). Graphene-based sensors usually use the conductivity of graphene or Dirac point of graphene (Sando et al. 2015; Ang et al. 2008). The conductivity

✉ Tianhong Cui
cuixx006@umn.edu

[1] Mechanical Engineering Department, University of Minnesota, 111 Church Street SE, Minneapolis, MN 55455, USA

[2] Department of Precision Instruments, Tsinghua University, Haidian District, Beijing, China

[3] ESIEE, University of Paris East, Paris, France

Published online: 25 October 2018

and Dirac point of graphene can be shifted by the amount of ions in the solution. Ion sensitive field effect transistor (IS-FET) is one of the graphene sensors. Therefore, graphene can be used as the sensing material to substitute the traditional colorimetric standard method because it has a number of merits such as low price, high sensitivity and selectivity.

To compete for the current standard colorimetric method as a good alternative, the minimum detection limit needs to be close to the current method. In addition, the sensor should have good selectivity which means the sensor can detect phosphate in the water without interference from other ions. First of all, phosphate selective membrane solution is synthesized and applied to the sensing area to detect phosphate in the water without interference from other ions. The polymer based phosphate selective membrane was synthesized by molecular imprinted technique (Haupt et al. 2012). The molecular imprinted polymer (MIP) has cavities in the polymer matrix which have an affinity to a specifically chosen template ion (Wulff 1995). In other words, the MIP, phosphate selective membrane, can only grab phosphate ions in the water. This means other ions such as nitrate, chloride and sulfate cannot penetrate the membrane and cannot give an effect on the graphene. To evaluate the sensor performance, the semiconductor analyzer is used with the several solutions that have different concentration and different ions in the measurement. The selective membrane is as important as the sensor fabrication to successfully detect phosphate ions in the water. Therefore, we focus on the fabrication process of the sensor using MEMs technique and the synthesis process of the phosphate selective membrane using molecular imprinting. Finally, we successfully show the ion selectivity and sensitivity of the IS-FET devices. The device fabrication process and the MIP solution synthesis process are well described in the experimental section. The device performance is also characterized in the results and discussion section.

2 Experimental

2.1 Preparation of graphene based sensor

Figure 1 shows the flow chart for the sensor fabrication. The first step is graphene growth. Graphene was synthesized by chemical vapor deposition (CVD) method. The synthesized graphene needs transfer to a target substrate with thermal release tape method (Caldwell et al. 2010). Traditionally, poly(methyl methacrylate) (PMMA) have been used in the transfer process followed by acetone clearing because PMMA can support large size graphene and obtain continuous graphene coverage (Suk et al. 2011). However, many research groups reported the disadvantage of PMMA (Gorantla et al. 2014). Although the continuous graphene sheet can be obtained by using PMMA, it is difficult to remove the polymer residue and transfer the graphene to the target location in the sensing area. The sequence is as follows, first to remove the protective film from the tape, then to put the adhesive part of the tape on the graphene sheet. The copper, catalyst substrate, is etched by a warm copper etchant (55–65 °C). The etching process takes 25 min for 25 μm. After etching the copper substrate, the film washes out several times with deionized (DI) water to remove the chemicals. The adhesion between the target substrate and graphene is a critical factor in successful graphene transfer. The target substrate, SiO_2, was treated with oxygen plasma for 15 min to enhance the adhesion (Kim et al. 2008). After the process, the tape on the substrate should be pressed softly to the substrate. To detach graphene from the tape, the substrate needs to be heated to about 100 °C. Although it is hard to obtain continuous graphene film with the thermal release tape method, this method can give fewer residues on the graphene sheet. After transferring graphene, the photoresist (S1813) was coated by spin-coater. Next, the coated photoresist was patterned with UV photolithography. The graphene was etched by using oxygen plasma etching on opened parts of photoresist. After removing the remained photoresist with acetone, Cr (30 nm) and Au (100 nm) were deposited by e-beam evaporation on the substrate to make Au electrodes. The deposited Au and Cr films were also patterned by the wet etching method, followed by coating and patterning photoresist. During the wet etching process, the etching time is very important to prevent from over etching. For the next layer, KMPR, a negative photoresist, was coated in the substrate, and then KMPR was patterned using photolithography. The last layer is the phosphate selective membrane. The synthesized membrane was coated by spin-coater (2000 rpm for 1 min), and the O-ring was attached to define the sensing area.

2.2 Preparation of selective membrane

Figure 2a shows the process of how to prepare the sensor with the phosphate selective membrane. The selective membrane is synthesized by molecular imprinting technique (MIP), which make cavities in the polymer like a stamping method (Warwick et al. 2014a, b). Since the polymerization of monomers was involved with templates in the process, the monomer will have the affinity for original molecules after removing the templates. Therefore, the MIP membrane can be used for the selective membrane. The solution for membrane was synthesized with cross-linking monomers [ethyleneglycoldimethacrylate (EGDMA) and polyurethane acylate (PUA)]. The ratio of

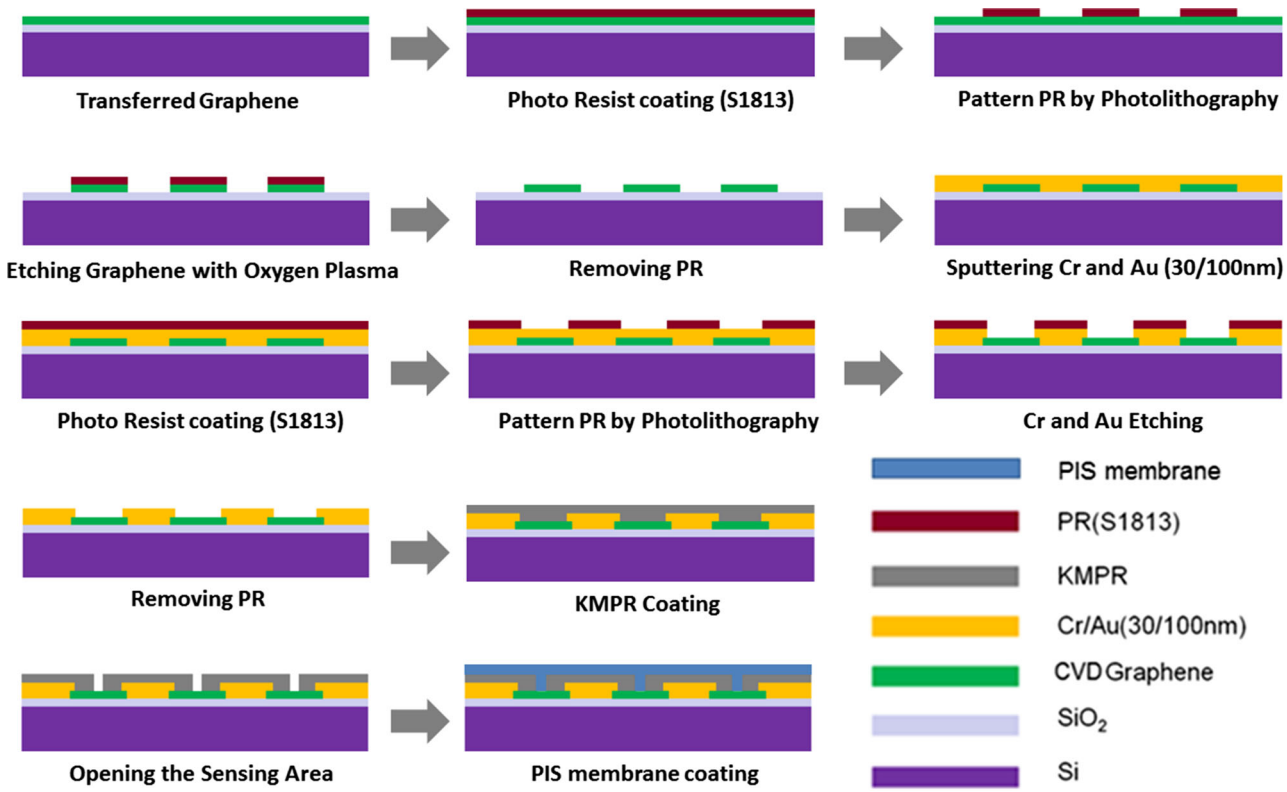

Fig. 1 The fabrication flow chart of the graphene based phosphate sensor

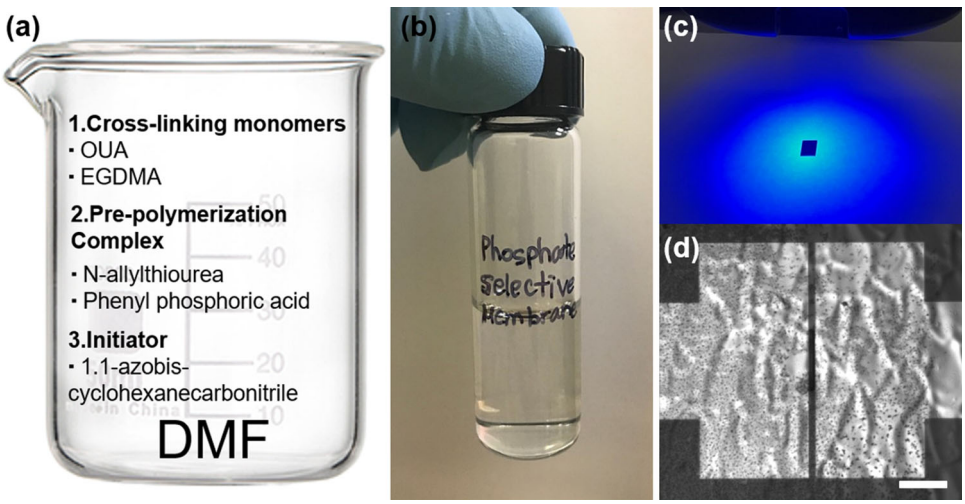

Fig. 2 **a** Synthesize process of the selective membrane solution, **b** synthesized selective membrane solution, **c** polymerization process with UV light, and **d** the optical image for the sensing area after coating the solution. The scale bar is 10 μm

cross-linkers was 85:15 to provide increased mechanical stability and flexibility. Thiourea was used for the monomer, and the template was phenylphosphonic acid. Cross-linkers [EGDMA (4.0 g) and PUA (0.71 g)], thiourea (0.59 g) and phenylphosphonic acid (0.40 g) were mixed with DMF solvent (2.44 g). Next, the initiator 1,1-azobis-cyclohexanecarbonitrile (0.07 g) was added in the mixture. Figure 2b shows the synthesized phosphate selective membrane solution that is transparent. The solution needs to be flushed with nitrogen gas to remove oxygen in the solution because the oxygen easily reacts with the free radicals and makes the solution polymerized. The synthesized solution was applied on the surface of the sensing area, and then the coated area was exposed to UV light (20 min) to polymerize the solution, as shown in Fig. 2c. Then, the polymerized membrane was rinsed with methanol to remove the phenylphosphonic acid templates from thiourea monomer. After washing the device, the surface of

the sensing area is characterized by optical microscope. Figure 2d is the optical image of the sensing area. The plasticized the solution shows the wrinkles on the surface. The membrane coated devices tested with different ion solutions, and the results are demonstrated in the measurement section.

2.3 Sensing mechanism

Figure 3a is the schematic diagram for the structure of graphene IS-FET. The device has three electrodes including source, drain and reference electrodes (Ahmad et al. 2013). The drain and the source electrode are connected with graphene and KMPR was coated on the surface of the device to cover Au electrodes and electrodes. The KMPR layer can prevent current from the leakage. The patterned KMPR has windows for graphene, which can make graphene expose to the solutions. Through this window the graphene can communicate with the solutions. For the last layer, the selective membrane was coated on the graphene. In the inset image in Fig. 3a, the final device has O-ring which can confine the ionic solutions. Figure 3b shows the mechanism of phosphate selective membrane. The selective membrane blocks other ions such as nitrate, chloride and sulfate in the solution, but only phosphate ions can penetrate the phosphate selective membrane, as shown in the Fig. 3b (Zhang et al. 2014). In other words, the phosphate ion can only give the doping effect on graphene. Therefore, IS-FET can get the selectivity by coating the selective membrane. In this experiment, the ion solutions with different ions were applied on the sensor to verify whether IS-FET shows the selectivity or not. In the measurement, the fixed voltage (0.05 V) was applied between source and drain electrodes (V_{DS}), while the reference voltage was swept from − 1 to 1 V. The transfer curve was obtained when the reference voltage was swept. The transfer curves were demonstrated in the next section.

3 Results and discussion

3.1 Fabricated sensor structure and transferred graphene

Figure 4a is the image of the fabricated sensor with 44 sensors on the Si/SiO_2 wafer. The KMPR was coated and patterned for the electrodes area and sensing area. The magnified inset image shows the sensing area. There is an opened KMPR window between the Au electrodes through which graphene can interact with the solution. The 10 graphene bridges are connecting two electrodes. The little dark parts in the bridges are the sensing area that is the KMPR window. The graphene can be exposed to the solution through this window. Raman spectroscopy was used to confirm the graphene layers. Figure 4b shows Raman spectroscopy of the transferred graphene on the Si/SiO_2 substrate. The Raman laser (532 nm) was focused on the graphene. The Raman spectroscopy shows the graphene bands (G band and 2D band) as well known in the previous study (Malard et al. 2009). G band and 2D band are located in the 1530 cm^{-1} and 2700 cm^{-1}, respectively. The result demonstrates that the graphene sheet does not get damaged during the several photolithography processes. After finishing the fabrication process, the selective membrane is coated on the graphene to cover the sensing area.

3.2 Measurement of the devices with the phosphate selective membrane

The IS-FET sensors were characterized by semiconductor analyzer because the doping type of graphene can be confirmed with the transfer curve (Papp et al. 2009). First, IS-FETs are tested without the membrane to check the effect of the selective membrane. The sensor shows a P-type property before coating the membrane. Because the graphene sheet got some damages and polymer residues during the transfer process (Regan et al. 2010). These damages make graphene P-type. In other word, holes are the main carriers in the graphene after finishing the

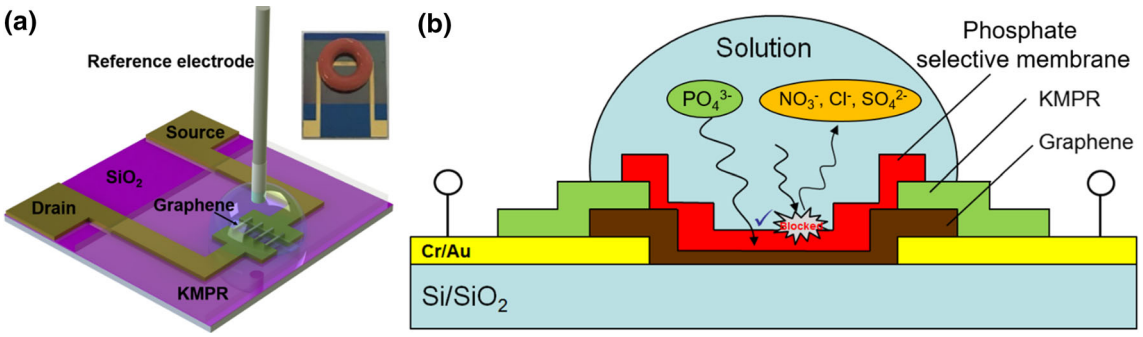

Fig. 3 **a** Schematic diagram for the structure of IS-FET, **b** schematic diagram for the mechanism of phosphate selective membrane

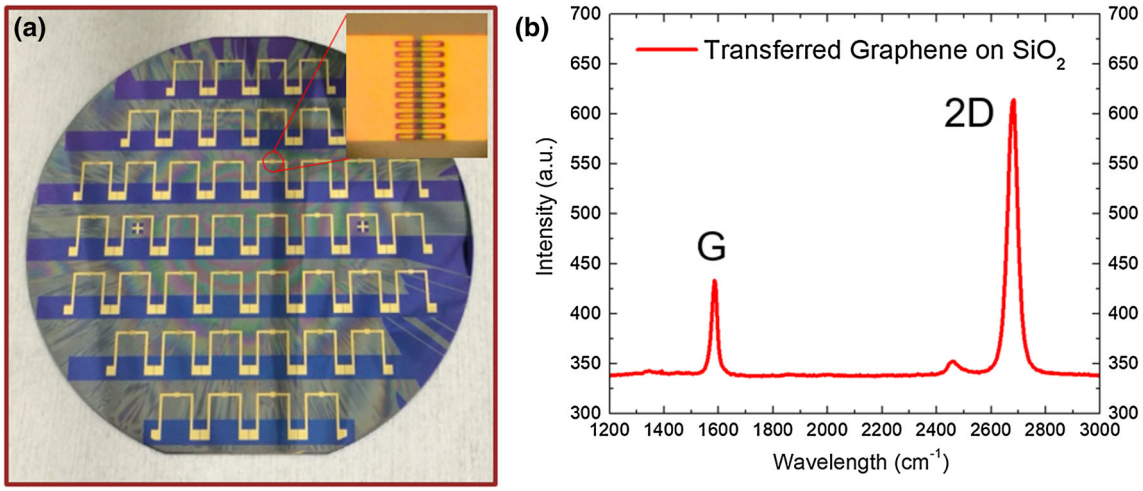

Fig. 4 **a** The wafer image after finishing KMPR patterning process, **b** Raman spectroscopy of graphene in the sensing region. The Inset image show the optical image of the sensing region

fabrication process. Therefore, Dirac point of the graphene is located in the positive side. However, the property is changed to N-type after coating the membrane. After coating the membrane, the main carrier is changed from holes to electrons in the graphene surface. The electrons are affected by the ions in the solution. The reason why the main carriers change is the presence of a charged ion in the polymer matrix that can attract the electrons in the graphene (Suedee et al. 2006). Figure 5 depicts the transfer characteristic of the sensor with selective membrane and without the membrane. In this figure, we confirm that the doping effects of graphene that come from the residue and the selective membrane. Dirac point is located in the positive side about 0.1 V before coating the membrane. However, it is shifted on the negative side about − 0.4 V.

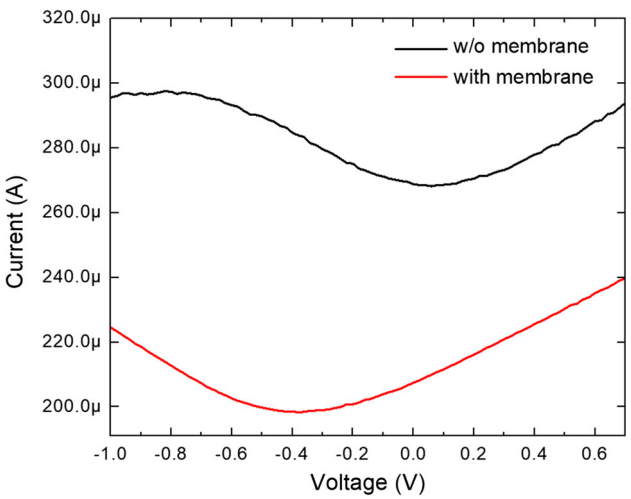

Fig. 5 Transfer curve of IS-FET with membrane and without membrane

And the overall current level is decreased due to the polymer membrane.

The membrane solution is coated by spin-coater (3000 rpm for 30 s). After coating the membrane, the sensor is tested with the phosphate solutions that have different concentration. Also, the other solutions (chloride, nitrate and sulfate) are applied to the sensor to confirm the selectivity of the sensors.

With the selective membrane, the main carrier of graphene, electrons, will be decreased as increasing the phosphate ions in water. Because the phosphate ions make the electrons in graphene repulse from the surface. This phenomenon causes the doping effect of graphene, making Dirac point shift to left or right. Therefore, the measurement of the Dirac point can be a great measurement method for detecting the amount of ions in water.

We applied the phosphate, chloride, nitrate, and sulfate solutions which have different concentrations (0, 0.1, 1 and 10 mg/L), and measure the responses of the FET devices to verify the function of the membrane. As increasing the concentration, the transfer curve shifts to the right side in both graphs. Without the selective membrane, the phosphate ions attract the holes in the graphene surface. After coating the membrane, the penetrated phosphate ions repel the electrons in the graphene surface. As a result, both transfer curves are shifted to the right side. The detection limit is 0.1 mg/L, and the response time is about 10 s. Each ion solution has four different concentrations (0–10 mg/L). Figure 6a shows the sensor response with chloride ion solution. As increasing the concentration, the Dirac point very slightly moves to left. However, the movement can be neglected. In Fig. 6b, the nitrate solutions were applied to the sensor. The nitrate solution could not make the Dirac point move as well. As shown in Fig. 6c, we can also

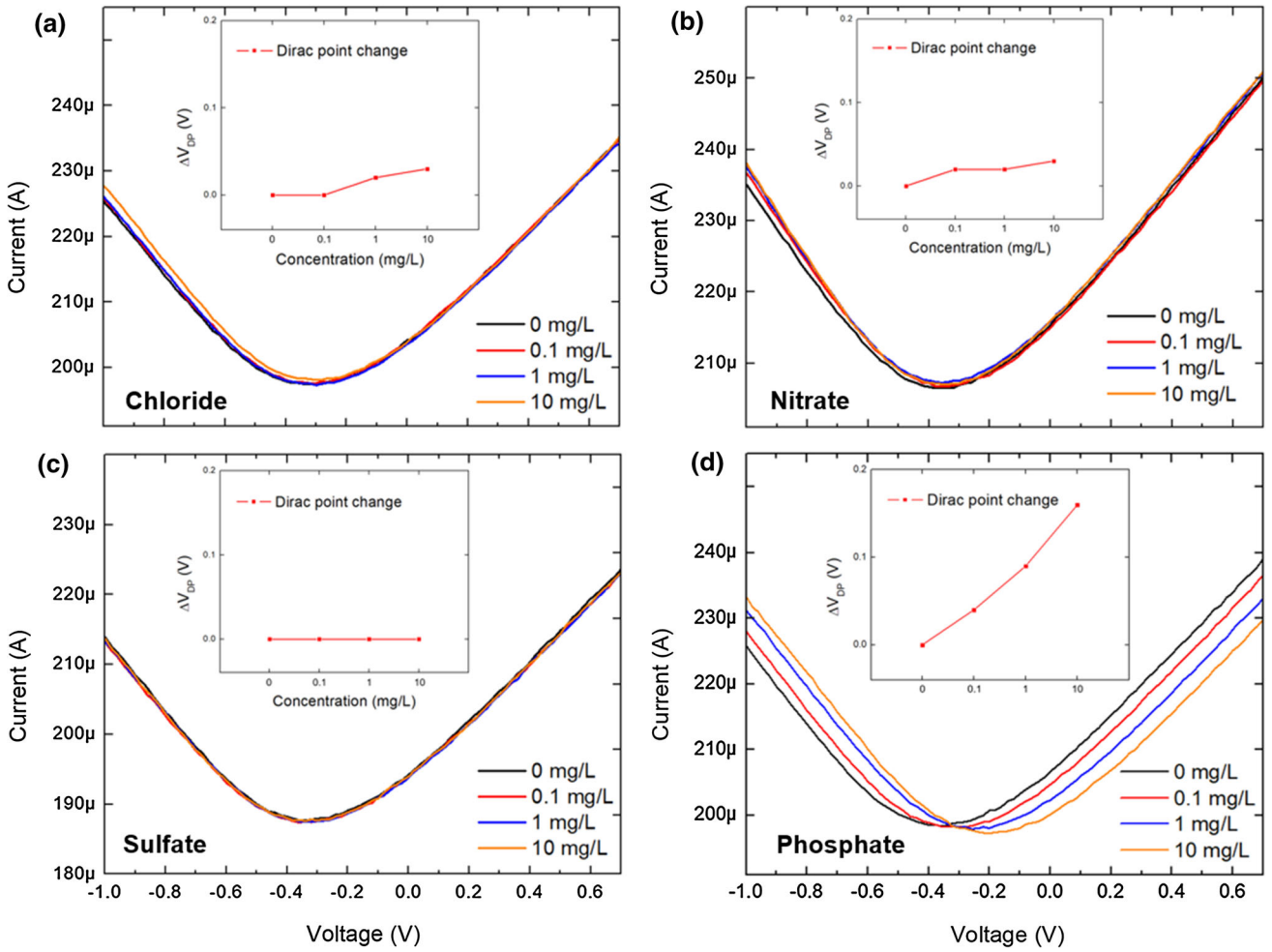

Fig. 6 Transfer curves of graphene IS-FET with phosphate selective membrane. Four different solutions were applied to the sensor. Each graph shows the sensor response with **a** chloride, **b** nitrate, **c** sulfate, and **d** phosphate solutions

confirm that sulfate ion cannot affect the sensor. Figure 6d shows the response sensor with phosphate ion solutions. In contrast with other solutions, the Dirac point was clearly shifted from left to right, as increasing the concentration.

The selectivity is the key factor of the sensor fabrication. Although the graphene sensor has high sensitivity with various ions in the solution, it does not have selectivity by itself. The synthesized phosphate selective membrane was applied to the sensor to give the sensor the selectivity. In other words, the devices can detect the phosphate without interference with other ions in the water, when the selective membrane is coated on graphene. The sensor deposited with the selective membrane was characterized to check the interference. In Fig. 7, the responses of the sensor were compared after applying various solutions with different ions and concentrations. The reference voltage at Dirac point was measured as increasing the concentration. The result shows that the sensor only responded with phosphate solutions. The Dirac points are shifted from − 0.4 to − 0.2 V with phosphate solutions. However, the sensor

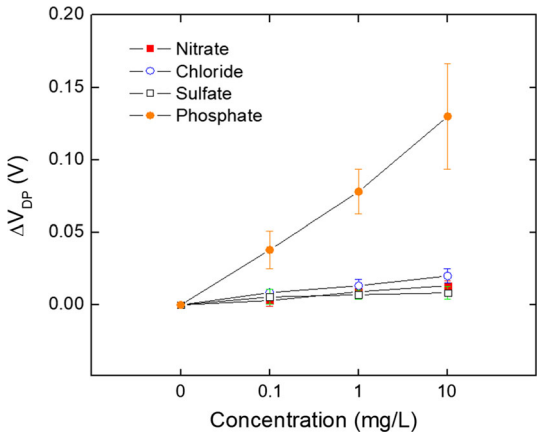

Fig. 7 Selectivity of the phosphate selective membrane

does not show a response with other solutions such as chloride, sulfate, and nitrate. As a result, we successfully confirm that the FET sensor has selectivity for phosphate solutions with the synthesized selective membrane. The

results show that IS-FET can be a promising candidate to substitute current colorimetric method.

4 Conclusions

The synthesized phosphate selective membrane was coated on the sensing area, and the sensors were characterized by semiconductor analyzer. Since Dirac point of graphene shifts to left or right side when it is affected by the doping effect, the sensor performance with the selective membrane was confirmed by measuring the shift of Dirac point of graphene with different ion solutions. We successfully synthesized the phosphate selective membrane and deposited the selective membrane to the sensor. Finally, the performance and selectivity of the IS-FET devices were successfully demonstrated. The Dirac point shifts from − 0.4 to − 0.2 V without the interference of other ions.

Acknowledgements The authors acknowledge the assistance of fabrication and characterization from Minnesota Nano Center and the Characterization Facility at the University of Minnesota.

References

Ahmad R, Tripathy N, Hahn YB (2013) High-performance cholesterol sensor based on the solution-gated field effect transistor fabricated with ZnO nanorods. Biosens Bioelectron 45:281–286. https://doi.org/10.1016/j.bios.2013.01.021

Ahn Y, Kim J, Ganorkar S, Kim YH, Kim SI (2016) Thermal annealing of graphene to remove polymer residues. Mater Express 6:69–76. https://doi.org/10.1166/mex.2016.1272

Ang PK, Chen W, Wee ATS, Kian PL (2008) Solution-gated epitaxial graphene as pH sensor. J Am Chem Soc 130:14392–14393. https://doi.org/10.1021/ja805090z

Caldwell JD, Anderson TJ, Culbertson JC, Jernigan GG, Hobart KD, Kub FJ, Tadjer MJ, Tedesco JL, Hite JK, Mastro MA, Myers-Ward RL, Eddy CR Jr, Campbell PM, Gaskill DK (2010) technique for the dry transfer of epitaxial graphene onto arbitrary substrates. ACS Nano 4:1108–1114. https://doi.org/10.1021/nn901585p

Cheng WL, Sue JW, Chen WC, Chang JL, Zen JM (2010) Activated nickel platform for electrochemical sensing of phosphate. Anal Chem 82:1157–1161. https://doi.org/10.1021/ac9025253

Dickman SR, Bray RH (1940) Colorimetric determination of phosphate. Ind Eng Chem Anal Ed 12(11):665–668. https://doi.org/10.1021/ac50151a013

Du J, Zhao L, Zeng Y, Zhang L, Li F, Liu P, Liu C (2011) Comparison of electrical properties between multi-walled carbon nanotube and graphene nanosheet/high density polyethylene composites with a segregated network structure. Carbon 49:1094–1100. https://doi.org/10.1016/j.carbon.2010.11.013

Geim AK, Novoselov KS (2007) The rise of graphene. Nat Mater 6:183–191. https://doi.org/10.1038/nmat1849

Gorantla S, Bachmatiuk A, Hwang J, Alsalman HA, Kwak JY, Seyller T, Eckert J, Spencer MG, Rümmeli MH (2014) A universal transfer route for graphene. Nanoscale 6:889–896. https://doi.org/10.1039/C3NR04739C

Haupt K, Linares AV, Bompart M (2012) Molecularly imprinted polymers. Top Curr Chem 325:1–28. https://doi.org/10.1007/978-3-642-28421-2

Her M, Beams R, Novotny L (2013) Graphene transfer with reduced residue. Phys Lett Sect A 377:1455–1458. https://doi.org/10.1016/j.physleta.2013.04.015

Kim H, Yoon B, Sung J, Choi DG, Park C (2008) Micropatterning of thin P3HT films via plasma enhanced polymer transfer printing. J Master Chem 18:3489–3495. https://doi.org/10.1039/B807285J

Kim J, Shin S, Kim YH, Kim SI (2014) Electrical coating method of graphene oxide. J Nanosci Nanotechnol 14:3658–3660. https://doi.org/10.1166/jnn.2014.7869

Kim J, Ganorkar S, Kim YH, Kim SI (2015) Graphene oxide hole injection layer for high-efficiency polymer light-emitting diodes by using electrophoretic deposition and electrical reduction. Carbon 94:633–640. https://doi.org/10.1016/j.carbon.2015.07.049

Liu Y, Dong X, Chen P (2012) Biological and chemical sensors based on graphene materials. Chem Soc Rev 41:2283–2307. https://doi.org/10.1039/C1CS15270J

Malard LM, Pimenta MA, Dresselhaus G, Dresselhaus MS (2009) Raman spectroscopy in graphene. Phys Rep 473:51–87. https://doi.org/10.1016/j.physrep.2009.02.003

Miao X, Tongay S, Petterson MK, Berke K, Rinzler AG, Appleton BR, Hebard AF (2012) High efficiency graphene solar cells by chemical doping. Nano Lett 12:2745–2750. https://doi.org/10.1021/nl204414u

Papp SB, Choi KS, Deng H, Lougovski P, van Enk SJ, Kimble HJ (2009) Characterization of multipartite entanglement for one photon shared among four optical modes. Science 324:768–771. https://doi.org/10.1126/science.1172260

Regan W, Alem N, Alemán B, Geng B, Girit Ç, Maserati L, Wang F, Crommie M, Zettl A (2010) A direct transfer of layer-area graphene. Appl Phys Lett 96:2008–2011. https://doi.org/10.1063/1.3337091

Sando S, Zhang B, Cui T (2015) A low-cost and label-free alpha-fetoprotein sensor based on self-assembled graphene on shrink polymer. In: 2015 28th IEEE international conference on micro electro mechanical systems (MEMS), pp 324–327. https://doi.org/10.1109/memsys.2015.7050954

Shin S, Kim J, Kim YH, Kim SI (2013) Enhanced performance of organic light-emitting diodes by using hybrid anodes composed of graphene and conducting polymer. Curr Appl Phys 13:144–147. https://doi.org/10.1016/j.cap.2013.01.016

Suedee R, Intakong W, Dickert FL (2006) Molecularly imprinted polymer-modified electrode for on-line conductometric monitoring of haloacetic acids in chlorinated water. Anal Chim Acta 509:66–75. https://doi.org/10.1016/j.aca.2006.03.081

Suk JW, Kitt A, Magnuson CW, Hao Y, Ahmed S, An J, Swan AK, Goldberg BB, Ruoff RS (2011) Transfer of CVD-grown monolayer graphene onto arbitrary substrates. ACS Nano 5:6916–6924. https://doi.org/10.1021/nn201207c

Tkachev SV, Buslaeva EY, Naumkin AV, Kotova SL, Laure IV, Gubin SP (2012) Reduced graphene oxide. Inorg Mater 48:796–802. https://doi.org/10.1134/S0020168512080158

Warwick C, Guerreiro A, Wood E, Kitson J, Robinson J, Soares A (2014a) A molecular imprinted polymer based sensor for measuring phosphate in wastewater samples. Water Sci Technol 69:48–54. https://doi.org/10.2166/wst.2013.550

Warwick C, Guerreiro A, Gomez-Caballero A, Wood E, Kitson J, Robinson J, Soares A (2014b) Conductance based sensing and analysis of soluble phosphates in wastewater. Biosens Bioelectron 52:173–179. https://doi.org/10.1016/j.bios.2013.08.048

Wulff G (1995) molecular imprinting in cross-linked materials with the aid of molecular templates—a way towards artificial

antibodies. Angew Chem Int Ed Engl 34:1812–1832. https://doi.org/10.1002/anie.199518121

Zhang Q, Wei F, Zhang S, Huang JQ, Peng HJ, Liu XY, Qian WZ, Wei F (2014) ionic shield for polysulfides towards highly-stable lithium–sulfur batteries. Energy Environ Sci 7:347–353. https://doi.org/10.1039/C3EE42223B

Zheng H, Smith RK, Jun YW, Kisielowski C, Dahmen U, Alivisatos AP (2009) Observation of single colloidal platinum nanocrystal growth trajectories. Science 324:1312–1314. https://doi.org/10.1126/science.1172104